Supporting Information

Xu et al. 10.1073/pnas.1205478109

S1. Feasibility of an active G-SERS substrate

S1.1 Permeability of the electromagnetic field through graphene

The permeability of the localized electromagnetic hot spots from the metal nanostructures to pass through a monolayer graphene is an essential step. The EM enhancement, approximately described by $I \propto \left|E_{loc} / E_0\right|^4$, is based on the greatly enhanced electromagnetic field caused by the localized surface plasmon resonance effect. First, through the extended Mie theory calculations as shown in **Fig. S1**, the localized electromagnetic fields between two gold nanospheres with and without a monolayer graphene shell are compared. It was found that the central electromagnetic field is even one order of magnitude stronger for Au@1LG than that for gold nanoparticles without 1LG, with the maximum value of $|E_{loc}/E_0|^2$ of 6.8×10^4 (***A***) and 4.5×10^3 (***B***), respectively. From the enlarged view in **Fig. S1*B***, the electromagnetic hot spot at the center of the nanosphere dimer can spread to the vicinity and pass across the monolayer graphene with good permeability.

Mie theory provides an analytical solution for the Maxwell equations but it is only capable for calculation of objects with a few regular geometries. To verify a case more similar to our G-SERS system, a system of two gold hemispheres adhering to a flat graphene surface was also studied by 3D-FDTD (three dimensional finite difference time domain) simulation (which allows the simulation of irregular nanostructures). **Fig. S2** shows the corresponding results. For a 60-nm gold hemisphere dimer with (**Fig. S2*A*, *C*, *E***) and without (**Fig. S2*B*, *D*, *F***) a monolayer graphene, their localized electromagnetic field distributions under a 632.8 nm incident laser were simulated. The "*E* intensity vs position" plot recorded the electric field distribution of the x-z plane (on the center of the gap between the gold hemisphere dimer, perpendicular to the graphene plane) and of the x-y plane (on top of the graphene with a distance of 0.16 nm, parallel to the graphene plane). We found that the maximum $|E_{loc}/E_0|^2$ value in the graphene contained structure (G-SERS structure) is even twice as large as that of the pristine gold hemisphere dimer.

The above theoretical results are intriguing that graphene seems to make the localized electromagnetic hot spots stronger. Actually in our earlier results dielectric shell coated sphere dimer was predicted to have an extremely high enhancement factor (1), in which a dielectric SiO_2 layer may introduce an additional enhancement through the multi-scattering processes. Here we think similar case may also exist in graphene shelled metal nanostructures and this aspect requires further studies. Thereby, it indicates that the localized electromagnetic hot spots can be introduced onto a flat graphene surface, and allows a G-SERS substrate to provide Raman enhancement with high sensitivity, comparable to (or even higher than) normal SERS.

S1.2 Raman signals of graphene as an inner indicator for the enhancement factor of a gold film

For simplicity and cleanliness, Au or Ag films deposited by vacuum thermal evaporation and monolayer graphene (1LG) samples prepared by mechanical exfoliation were first used for our G-SERS tests. It should be mentioned that, graphene itself is a good Raman probe with stable and intrinsic Raman signals. Thus, a series of different thicknesses of gold films deposited on 1LG were prepared, to compare their SERS activity. As shown in **Fig. S3**, compared to pristine graphene samples, the Raman signal of 1LG was greatly enhanced by the deposition of a gold film, and the enhancement varied with the thickness of the gold films from 0, 1, 3, 5, 8, 10, 15 to 20 nm. **Fig. S3** further shows that the maximum enhancement occurs for a thickness of 8 nm. Thicker gold films would remarkably absorb the incident laser and bury the graphene sample, and thus both the visibility and the Raman signal of graphene will decrease. For instance, when a 20 nm gold film was deposited, the Raman signals of both the 1LGs and the graphite pieces are almost invisible. **Fig. S4** shows the SEM images of 1, 3, 5, 8, 10, 15 and 20 nm gold films on a SiO_2/Si substrate for regions with and without monolayer graphene, together with the corresponding absorption spectra (panel (***H***)) in the visible region of gold films deposited under the same conditions on glass. A red shift of the maximum absorption peak frequency with the increase of the thickness of gold films is observed from the absorption spectra. From the SEM images (panel ***A*** to ***G***), we can see that the size and density of the gold islands increased with the thickness of the gold film, and for each thickness, gold on 1LG seems rougher than that on the SiO_2/Si substrate, which is related with the surface energy of graphene (2, 3).

S2. Spectral features of R6G

For comparison, graphene enhanced Raman scattering (GERS) spectra of R6G (1LG/R6G) are shown in **Fig. S5** as a supplement for **Fig. 2*B*** in the text. The main Raman features and their assignments (4,5) of the GERS, G-SERS(Au), G-SERS(Ag), SERS(Au), G-SERS(Ag) spectra of R6G are listed in **Table S1**.

It should be mentioned that the Raman signals of R6G for SERS(Au) and SERS(Ag) are irreproducible for themselves. Detailed experiments of parallel measurements of R6G with SERS(Au) and SERS(Ag) are shown in **Fig. S6**.

S3. G-SERS tapes: fabrication and spectroscopic characterization

S3.1 Large area and high quality monolayer graphene grown on a copper foil by the CVD method

CVD-grown graphene on a copper foil was chosen to replace the mechanically exfoliated graphene because of its large scale uniformity and high quality. **Fig. S7*A*** and ***B*** show an optical image and the corresponding Raman spectra of our synthesized graphene samples prepared by the chemical vapor deposition (CVD) method. The sample was transferred onto a SiO_2(300nm)/Si substrate, which is uniform over a large size, containing a monolayer structure.

S3.2 G-SERS tapes fabricated using exfoliated graphene

It should be mentioned that, exfoliated graphene samples can also be fabricated into such a G-SERS tape for extended applications. **Fig. S8** shows a similar experiment for the detection of a self-assembled monolayer of *p*-aminothiophenol showing its characteristic Raman peaks at 1074 and 1172 cm^{-1} (Panel (***C***)). Panel (***A***) and (***B***) show the optical images of a 1LG on SiO_2/Si substrate and after fabricating this substrate into a self-supporting structure, respectively. The alphabetic markers on the SiO_2/Si substrate were duplicated onto the PMMA film and these markers will benefit for locating the graphene covered regions for G-SERS measurements. Comparison between the G-SERS and the pristine Raman spectra show that the G-SERS tape fabricated using exfoliated graphene is also an effective substrate for G-SERS measurements. This approach will enable other 2D atomic crystals to be exploited for the fabrication of a similar kind of SERS substrate when their scaled production techniques are not available.

S3.3 G-SERS tapes fabricated using silver as an electromagnetic enhancer

Here we also demonstrated the fabrication and applications of active G-SERS tapes using silver as an electromagnetic enhancer. The procedure can be similar to G-SERS(Au) as mentioned in the text, but since silver is a more chemically-active species than gold, G-SERS(Ag) tapes needs to be fabricated with a few modifications as will be described in the following. First, an inert Al_2O_3 layer (with a thickness of 2 nm, prepared by the atomic layer deposition (ALD) technique) is introduced between the silver film and the PMMA layer. The existence of Al_2O_3 can stop the Ag-PMMA contact (which will cause additional signals and make the baseline complicated) as well as make the silver nanoislands more stable. Second, CVD grown graphene on copper should be transferred onto another substrate such as an aluminum foil or a SiO_2/Si substrate. The silver is more easily oxidized and the Fe^{3+} etching step in a G-SERS(Au) fabrication procedure may partly etch the silver (the reduction potential of Ag^+ is close to Fe^{3+}). Thus, when an aluminum foil or a SiO_2/Si substrate was used as the "sacrificial substrate", G-SERS(Ag) tapes can be achieved by etching them easily (for example, with an HCl solution for aluminum and KOH solution for SiO_2) without affecting the silver nanoislands.

The gapped nanostructures are responsible for a sensitive G-SERS substrate. First we characterized the morphology of a vacuum thermal deposited 8 nm silver film with transmission electron microscopy (TEM) (**Fig. S9**). Even though the gaps between nanoislands are larger than that of the gold, among them many are less than 5 nm, and quite a few are even less than 2 nm (**Fig. S9*B***). SEM images of a G-SERS(Au) tape and an as-prepared G-SERS (Ag) tape are shown in **Fig. S10**. The appearance of gold and silver in a G-SERS tape is more or less changed (especially for silver) from that of a pristine metal film during the drying of PMMA layer, yet very close dimers and aggregates can be found, to guarantee a considerable electromagnetic enhancement. Further we checked the Raman enhancement activity of the G-SERS(Ag) tape. As shown in **Fig. S11**, we succeeded in the detection of a 1×10^{-6} M aqueous solution of crystal violet (CV). The pristine CV solution under a PMMA tape shows a fluorescence background without distinguishable vibrational information of the molecules, and under the presence of monolayer graphene (PMMA/1LG, which can be called a "graphene tape"), the Raman signals of CV are observed with a bad signal-to-noise ratio

(and the Raman signal of graphene itself is almost invisible). In contrast, G-SERS(Ag) spectra show clear vibrational bands for both CV and graphene with a high signal-to-noise ratio.

S3.4 A way to overcome the surface vibration problem during in-situ measurements on the surface of a solution

It should be mentioned that the surface vibration problem causes troubles in a G-SERS study of a solution surface. Supposing that the sample under a focused laser spot is moving from one position to another during spectral acquisition (**Fig. S12*A***), the resulting Raman spectra will inevitably contain artifacts and the real signal may be buried within the changing background. Accordingly, here we found a good solution to this problem. When putting a 1 cm-diameter glass tube around the G-SERS tape (**Fig. S12*B***), it will totally remain stationary in such a restricted space, which enables measurements to be made with long-time acquisition.

S3.5 Extended applications of the G-SERS tapes in non-aqueous systems

In our experiments, it is found that the self-supporting G-SERS tape can spontaneously spread on the surface of water (or aqueous solutions), with the PMMA side facing upwards. Direct contact between the G-SERS-active face and the solution allows in-situ Raman spectroscopy measurements to be made. However, this procedure may not be applicable in non-aqueous solutions. For an as-prepared G-SERS tape without modification as described below, the tape may sink at once if the solvent is ethanol. We try to prevent the G-SERS tape from sinking by just sticking a “life buoy” to the tape (using a piece of foam plastic with a window in the middle). As shown in **Fig. S13**, we succeeded in detecting CuPc in ethanol with a G-SERS(Au) tape floating on the surface of a 1×10^{-5} M solution. A strong Raman signal of CuPc was obtained in G-SERS (black line), while only the weak Raman signal of ethanol was observed in the pristine spectrum (red line).

References

1. Xu HX (2004) Theoretical study of coated spherical metallic nanoparticles for single-molecule surface-enhanced spectroscopy. *Appl Phys Lett* 85(24):5980-5982.
2. Luo ZT, *et al.* (2010) Size-selective nanoparticle growth on few-Layer graphene films. *Nano Lett* 10:777-781.
3. Zhou HQ, *et al.* (2010) Thickness-dependent morphologies of gold on N-layer graphenes. *J Am Chem Soc* 132:944-946.
4. Hildebrandt P, Stockburger M (1984) Surface-enhanced resonance Raman spectroscopy of Rhodamine-6g adsorbed on colloidal silver. *J Phys Chem* 88:5935-5944.
5. Majoube M, Henry M (1991) Fourier-transform Raman and infrared and surface-enhanced Raman spectra for Rhodamine-6g. *Spec Acta A-Mol Biomol Spec* 47:1459-1466.

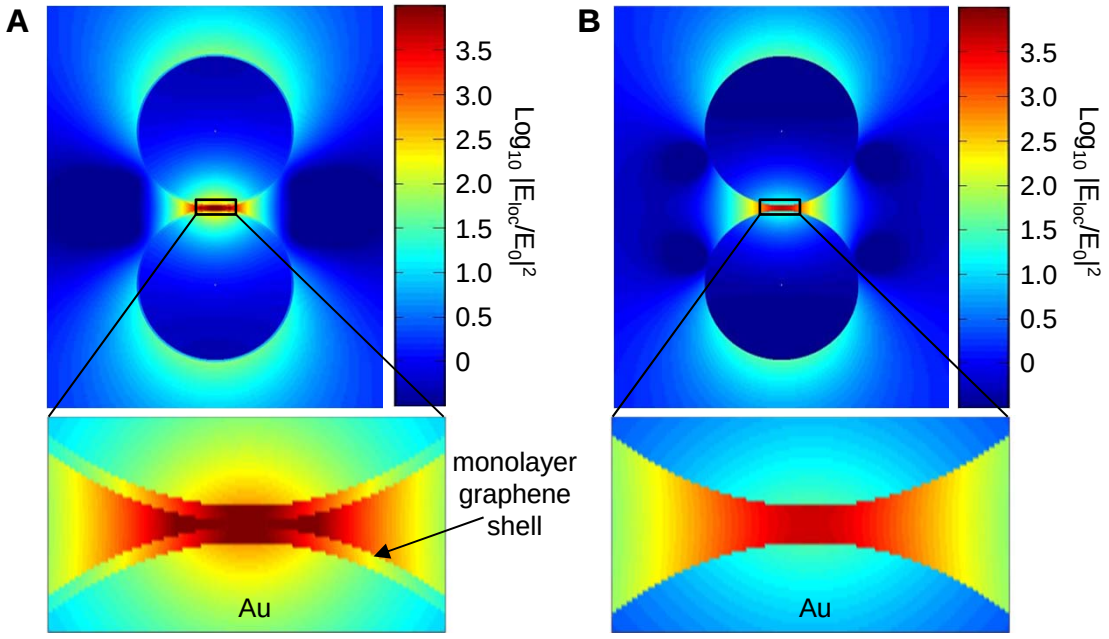

Fig. S1 Spatial distribution of the electromagnetic field between two 60-nm gold nanospheres calculated using extended Mie theory. (*A*,*B*) Gold nanoparticles coated with (*A*) and without coating (*B*) of a monolayer graphene shell. The maximum values of $|E_{loc}/E_0|^2$ for (*A*) and (*B*) are 6.8×10^4 and 4.5×10^3, respectively. Enlarged regions are shown to visualize the region between the two nanoparticles. The distance between the two gold nanoparticles is 2 nm, the thickness of the graphene shell is 0.34 nm (with 0.5 nm vacuum between graphene coating layer and a gold sphere). The distance between the two graphene shells in (*A*) is 0.32 nm. The excitation wavelength is 632.8 nm.

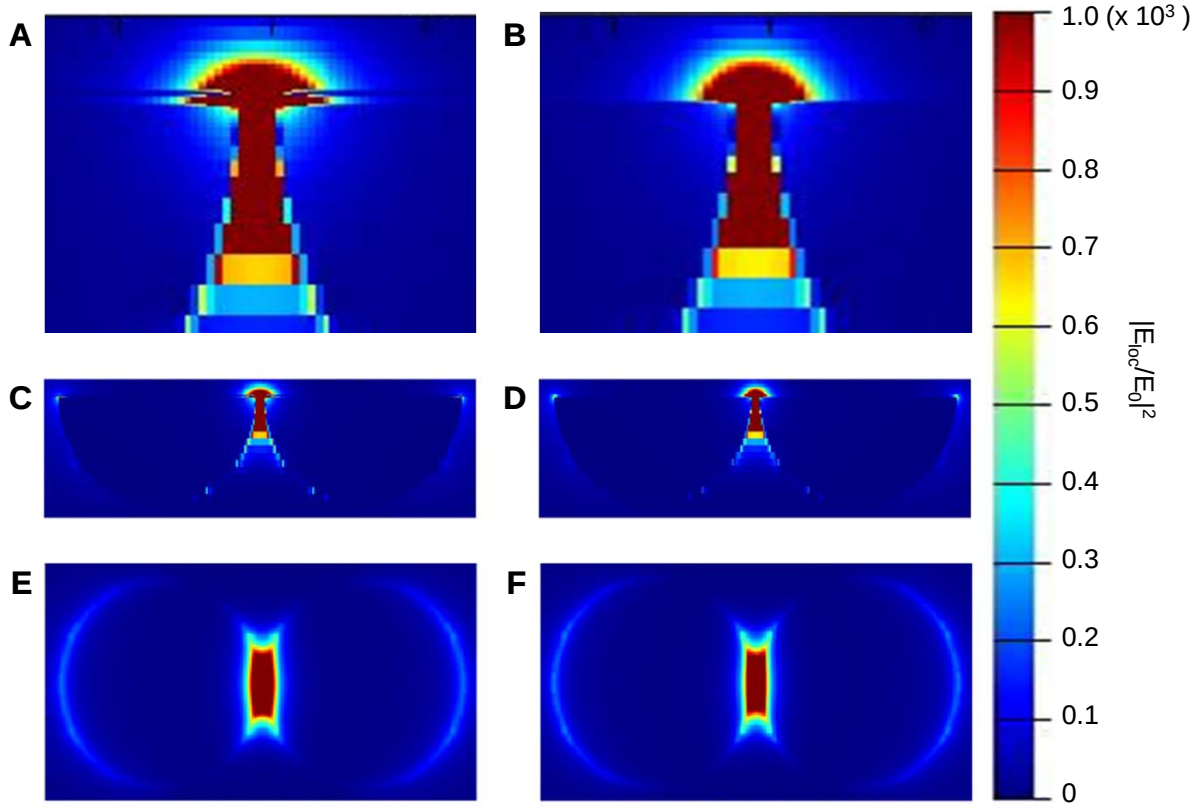

Fig. S2 3D-FDTD simulation of a 60-nm gold hemisphere dimer with (*A*, *C*, *E*) and without (*B*, *D*, *F*) graphene (with a 2-nm gap between two gold hemispheres and a 0.5-nm gap between gold hemispheres and graphene). (*A-D*) The "$|E_{loc}/E_0|^2$ vs position" plot of the x-z plane (on the center of the gap between the gold hemisphere dimer, perpendicular to the graphene plane), (*A*) and (*B*) are enlarged views of the hot spot in (*C*) and (*D*). Maximum $|E_{loc}/E_0|^2$ is 4.3 x 10^4 in (*A*) and (*C*), and 2.5 x 10^4 in (*B*) and (*D*). (*E*, *F*) The "$|E_{loc}/E_0|^2$ vs position" plot of the x-y plane on top of graphene (distance = 0.16 nm). Maximum $|E_{loc}/E_0|^2$ is 4.6 x 10^3 in (*E*), and 4.2 x 10^3 in (*F*).

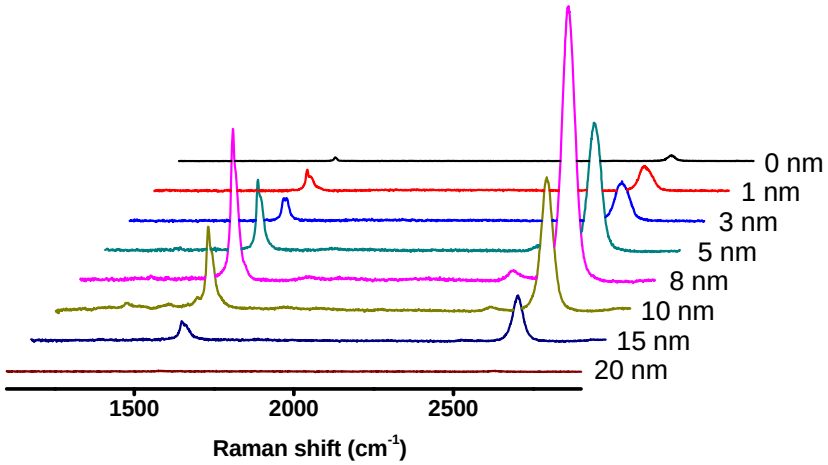

Fig. S3 Enhanced Raman spectra of 1LG with the deposition of different thicknesses of gold films. The intensity evolution of the G-band (~1580 cm^{-1}) and G'-band (~2630 cm^{-1}) for 0, 1, 3, 5, 8, 10, 15, 20 nm gold films indicates a preferred thickness of 8 nm, which provides the largest enhancement for the Raman signal of graphene. Every spectrum was taken using a 10 s exposure, one-time acquisition and a 0.7 mW laser power under a 632.8 nm laser excitation.

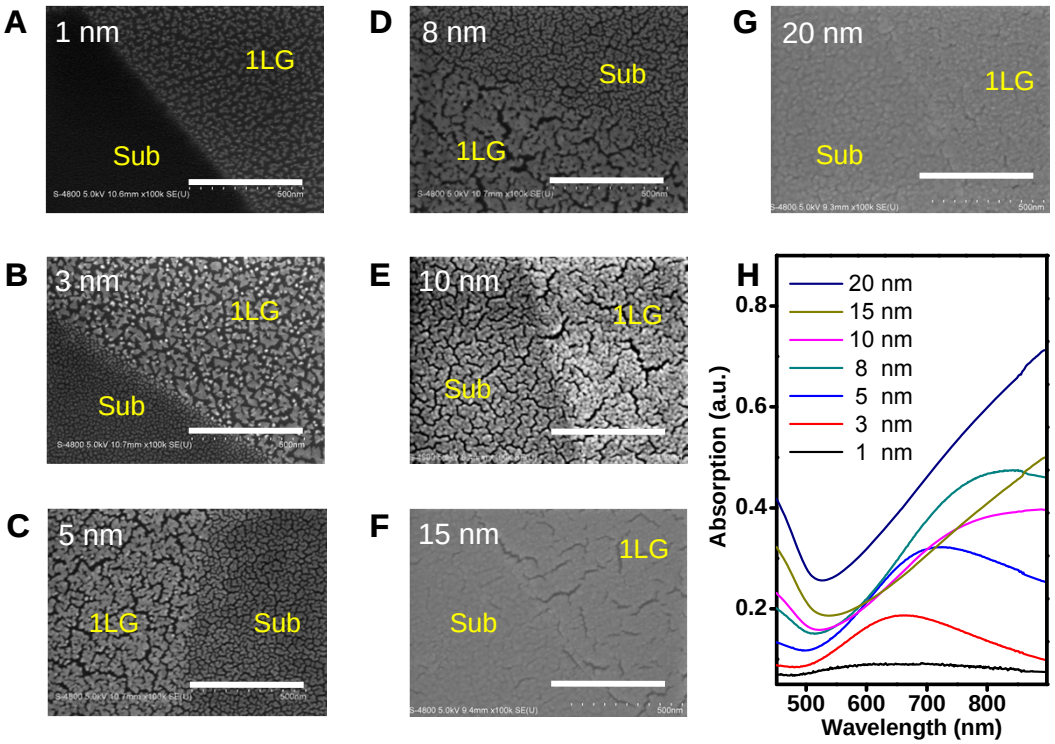

Fig. S4 SEM images of different thicknesses of gold films. (*A-G*) Different thickness of gold films deposited on exfoliated 1LG pieces on a SiO_2/Si substrate. "1LG" and "Sub" correspond to a gold film on a SiO_2/Si substrate for regions of with and without the 1LG. The scale bar is 500 nm. (*H*) The corresponding absorption spectra of the same thicknesses of gold films deposited on glass. Maximum absorption positions for 1, 3, 5, 8 nm gold films are around 657 nm, 663 nm, 717 nm and 830 nm, respectively, and the absorption of thicker gold films shifts to the near-infrared spectral region.

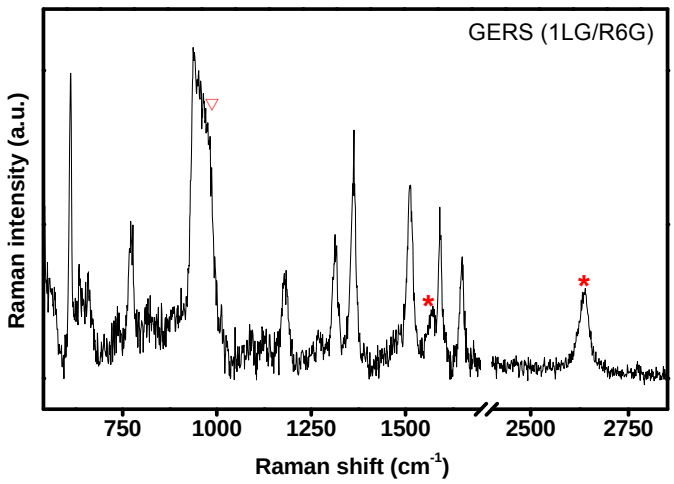

Fig. S5 GERS spectra of R6G (1LG/R6G) on a SiO_2(300nm)/Si substrate. "▽" and "*" mark peaks that are from the SiO_2/Si substrate and monolayer graphene, respectively.

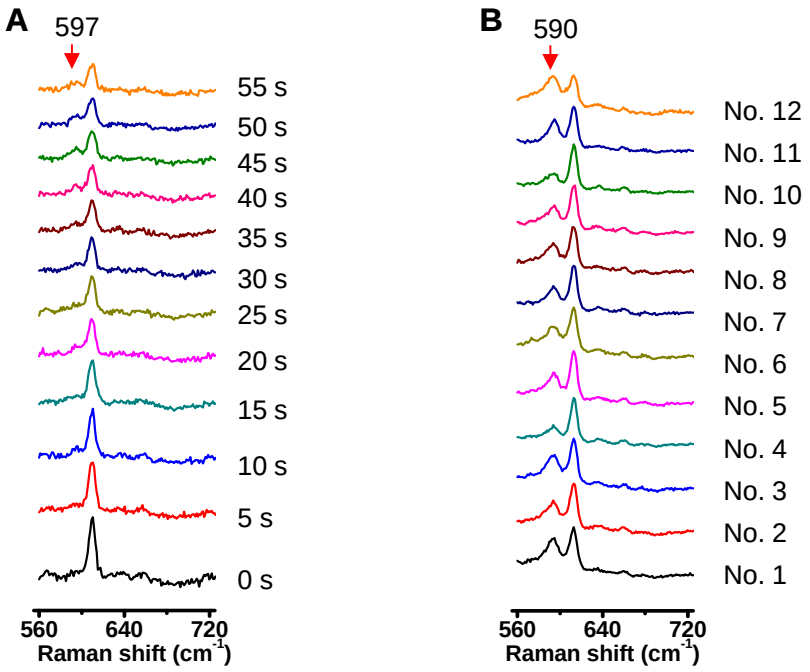

Fig. S6 The reproducibility of the ~597 cm^{-1} peak of R6G measured by SERS(Au) (*A*) and the ~ 590 cm^{-1} peak of R6G measured by SERS(Ag) (*B*). (*A*) A continuous time series of 12 spectra measured at a same position in the SERS(Au) region under the same conditions (every spectrum with a 5 s acquisition), it seems that something turned up at 10 s, but it became clear until at 40 s, yet its intensity and appearance is changing. (*B*) 12 spectra of parallel measurements of R6G in SERS(Ag) regions at different positions of a same sample. We found that the ~590 cm^{-1} peak is relatively low for No. 4 and No. 10, also their intensity and band shift can be varied from one another.

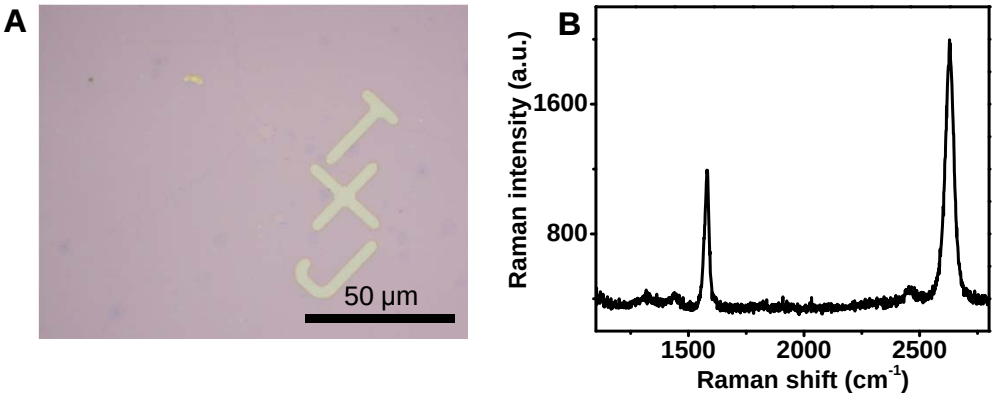

Fig. S7 Optical image (*A*) and Raman spectra (*B*) of a CVD-grown monolayer graphene film, which was grown from a copper foil and transferred to a SiO_2(300 nm)/Si substrate.

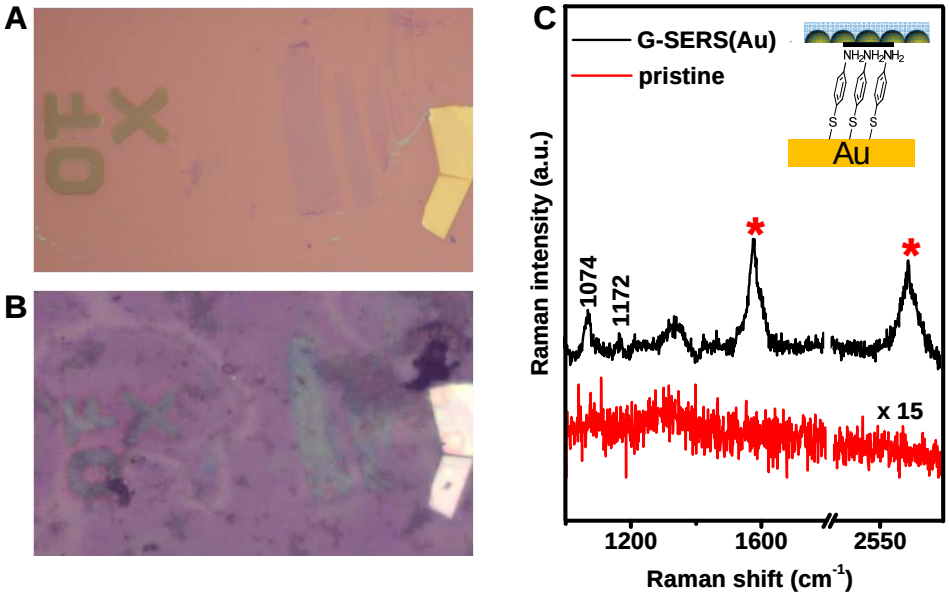

Fig. S8 A G-SERS tape made from exfoliated graphene for detection of a self-assembled monolayer of *p*-aminothiophenol. (*A*,*B*) optical images of 1LGs on SiO_2/Si (*A*) and after fabricated into a free-standing tape (*B*). (*C*) The corresponding G-SERS and pristine Raman spectra of a self-assembled *p*-aminothiophenol monolayer. (Inset shows the corresponding representation of our sample structure. The G-SERS tape made from exfoliated graphene is shown on the top.) "*" marks the G-band and G'-band of monolayer graphene.

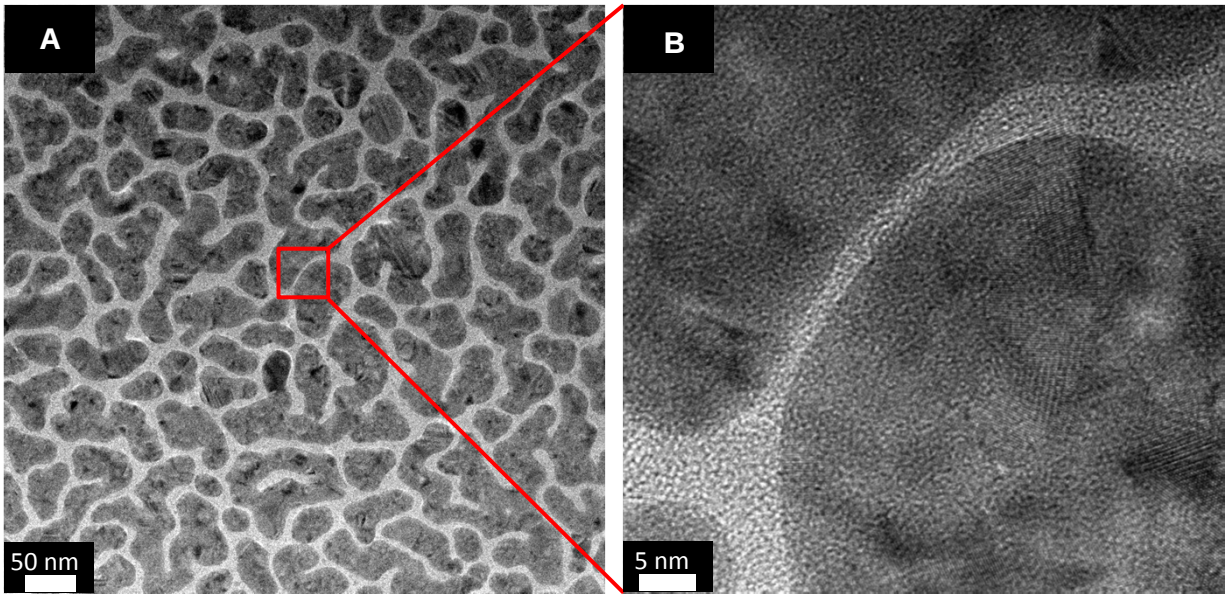

Fig. S9 TEM characterization of an 8-nm silver film. (*A*) A global view. (*B*) An enlarged view of a 2-nm gap of a nanoisland dimer. The silver film was deposited directly on a copper grid with by vacuum thermal deposition.

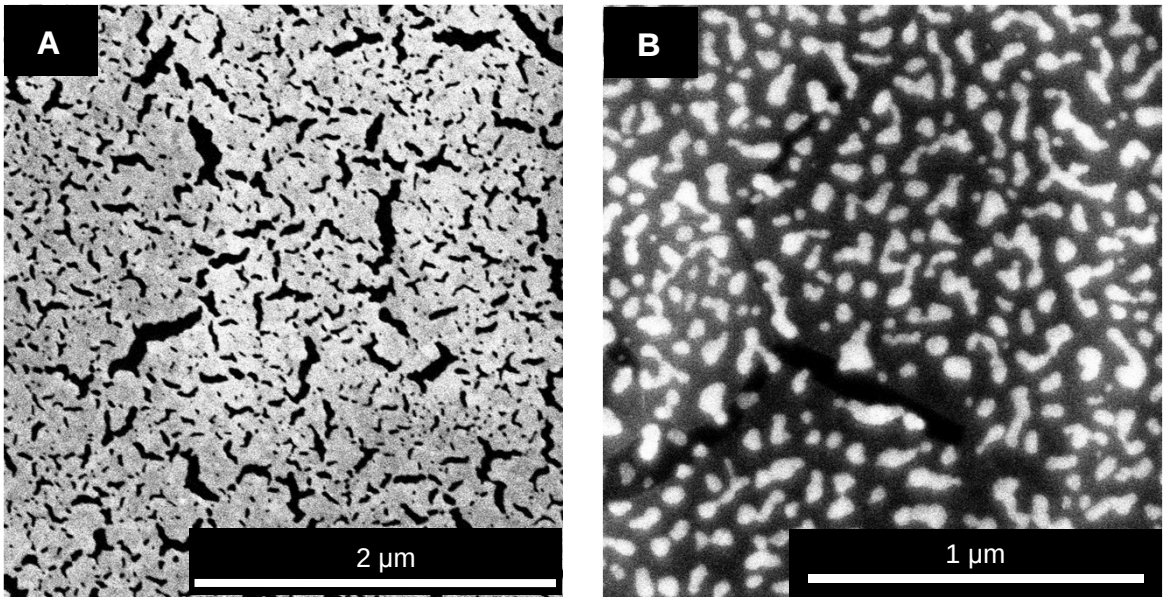

Fig. S10 SEM images of a G-SERS(Au) tape (*A*) and a G-SERS(Ag) tape (*B*). The gold/silver nanoislands are shown with the flat surface facing upwards, which are buried under a monolayer graphene.

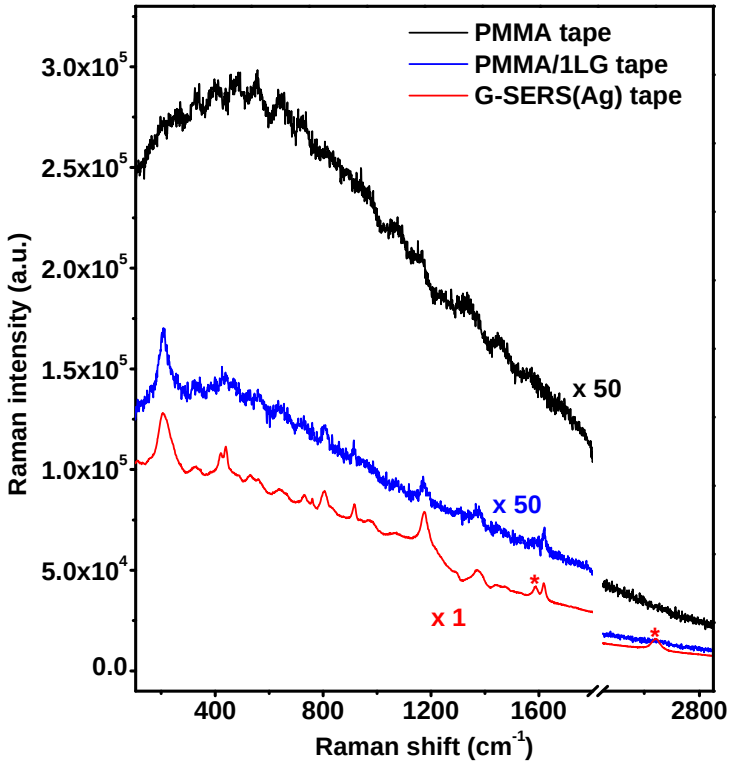

Fig. S11 Raman measurement with a G-SERS(Ag) tape floating on the surface of a 1×10^{-6} M aqueous solution of crystal violet (red line). The other two spectra are parallel experiments with only PMMA (black line) and PMMA/1LG (blue line, can be called a "graphene tape"). "*" marks the G-band and G'-band of monolayer graphene.

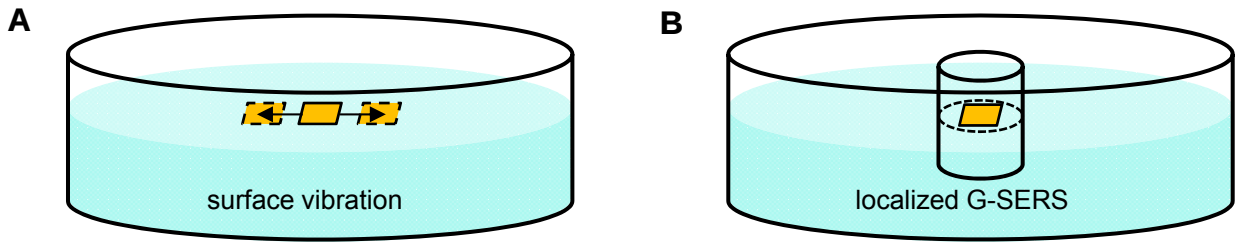

Fig. S12 The surface vibration problem of a G-SERS tape on the surface of a solution (*A*) and a feasible solution (*B*) by the addition of a 1 cm-diameter glass tube around the tape.

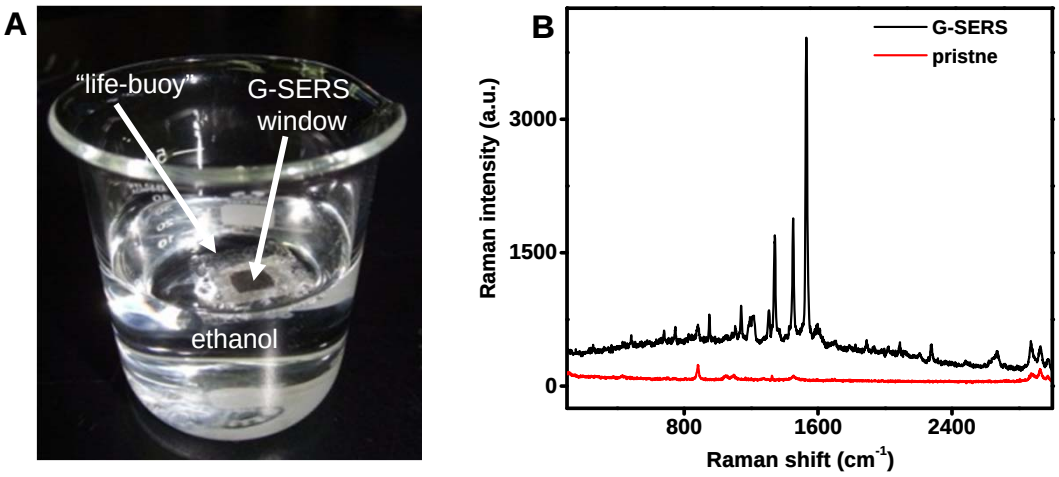

Fig. S13 Modified G-SERS tape for CuPc detection in ethanol. (*A*) A modified G-SERS tape floating on the surface of ethanol. (*B*) G-SERS (taken from a G-SERS tape with a "life buoy") and pristine Raman spectra on the surface of a CuPc solution in ethanol. Red and black lines in panel (*B*) are from the pristine and G-SERS results, respectively. The CuPc solid was first dissolved in CF_3COOH:CH_2Cl_2 (1:10, V:V) to 4×10^{-4} M, and then diluted to 1×10^{-5} M with ethanol.

Table S1 Band positions (in cm^{-1}) and their assignments observed for GERS, G-SERS(Au), G-SERS(Ag), SERS(Au), SERS(Ag) spectra of R6G. "*" marks Raman signals from the monolayer graphene.

GERS	G-SERS(Au)	G-SERS(Ag)	SERS(Au)	SERS(Ag)	Tentative assignments
				554	
			597	590	
612	613	612	612	608	xanthene ring deformation (XRD)
635	634	635	635	635	
659	660	660	660	657	
772	772	771	772	768	XRD
			1014	1012	external group mode (EGM)
1181	1182	1181	1186	1182	
1313	1313	1313	1314	1312	C-H deformation
				1336	
1362	1361	1361	1360	1359	xanthene ring stretching (XRS)
			1411	1403	EGM ethylamino groups
			1468	1471	
1511	1511	1511	1510	1507	XRS
			1540	1531	EGM
1571*	1570*	1568*	——	——	G-band of 1LG
			1574	1575	XRS
1591	1590	1589	1600	1595	XRS
1649	1648	1648	1646	1643	XRS
2637*	2626*	2624*	——	——	G'-band of 1LG